J. Cosmet. Sci., **65,** 37–48 (January/February 2014)

Preliminary analysis of the distribution of water in human hair by small-angle neutron scattering

YASH KAMATH, N. SANJEEVA MURTHY, and
RAM RAMAPRASAD, *Kamath Consulting Inc., Monmouth Junction, NJ (Y.K.), Center for Biomaterials Rutgers University, Piscataway, NJ (N.S.M), and TRI/Princeton, Princeton, NJ (R.R.).*

Accepted for publication November 17, 2013.

Synopsis

Diffusion and distribution of water in hair can reveal the internal structure of hair that determines the penetration of various products used to treat hair. The distribution of water into different morphological components in unmodified hair, cuticle-free hair, and hair saturated with oil at various levels of humidity was examined using small-angle neutron scattering (SANS) by substituting water with deuterium oxide (D_2O). Infrared spectroscopy was used to follow hydrogen–deuterium exchange. Water present in hair gives basically two types of responses in SANS: (i) interference patterns, and (ii) central diffuse scattering (CDS) around the beam stop. The amount of water in the matrix between the intermediate filaments that gives rise to interference patterns remained essentially constant over the 50–98% humidity range without swelling this region of the fiber extensively. This observation suggests that a significant fraction of water in the hair, which contributes to the CDS, is likely located in a different morphological region of hair that is more like pores in a fibrous structure, which leads to significant additional swelling of the fiber. Comparison of the scattering of hair treated with oil shows that soybean oil, which diffuses less into hair, allows more water into hair than coconut oil. These preliminary results illustrate the utility of SANS for evaluating and understanding the diffusion of deuterated liquids into different morphological structures in hair.

INTRODUCTION

Hair is a part of skin, a protective organ of most mammals. It consists of mainly keratin, a structural protein that is also a major constituent of hoofs, nails, and horns. Although hair has a molecularly complex hierarchical structure (Fig. 1) (1), three distinct parts can be identified in the cross sections of human hair fibers: the cuticle, the cortex, and the medulla (2). The cuticle sheath, which is the outermost protective layer, consists of several layers of cuticle cells arranged like shingles on a roof. The cuticle envelopes the cortex, which is made of cortical cells that comprise the major part of the α-keratin in hair. Cells in both the cuticle and the cortex are held together by cell membrane complexes. Cells in the cortex occur as an assemblage of macrofibrils with rodlike intermediate filaments

Address all correspondence to Yash Kamath at yashkamath@verizon.net.

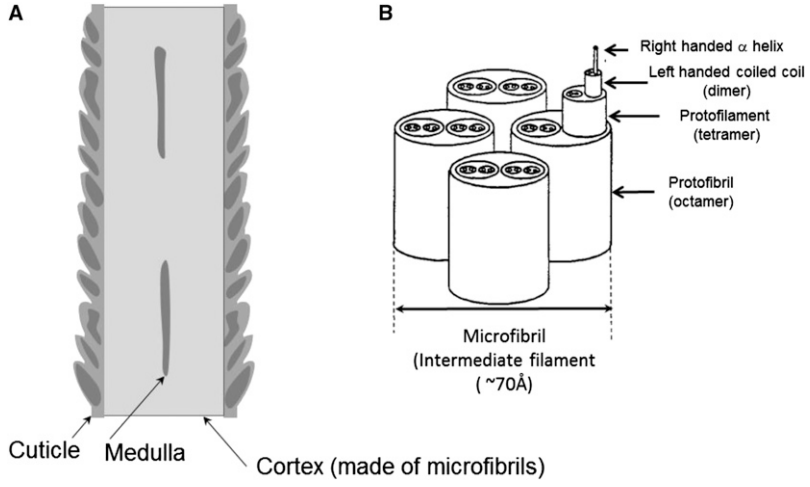

Figure 1. (A) Schematic of the longitudinal section of hair shaft, (B) A model for the internal organization of the keratin molecules in the microfibril.

(IFs, sometimes referred to as microfibril) embedded in an amorphous matrix of keratin-associated proteins cross-linked by the amino acid cystine. The IFs are made of eight protofilaments, each with a pair of coiled-coil α-keratin molecules, and thus contains 32 α-helical chains. The medulla, which can be sometimes found in the cross section, is a structure made of incompletely developed hollow cells. IF and the surrounding matrix constitute about 85% of the hair shaft, but the properties of hair are determined by all the constituents that make up hair (3). This paper presents observations about the ingress of water and its distribution into the different structures of hair.

The mechanical properties of hair, such as tensile strength, bending, and torsional rigidity, are sensitively dependent on the amount of water in the fiber (4). Hair, with a hydrophilic core and a hydrophobic surface, absorbs water from the vicinity, the amount depending on the relative humidity (RH) of the environment. The longitudinal swelling of hair with moisture content is the basis of hygrometer used for the measurement of RH in the environment (2). Water molecules diffuse into the fiber through intercellular pathways, such as the cell membrane complexes, rather than transcellular pathways. The fiber equilibrates rather slowly to the partial pressure of water vapor in the environment. This behavior has been studied and quantified in detail, using dynamic vapor sorption analyzer (Surface Measurements Systems, Alperton, Middlesex, U.K.) (5). This apparatus gravimetrically determines the amount of water absorbed by hair from the moisture surrounding the hair sample as a function of RH. Desorption data can also be obtained in the same experiment by reversing the steps. From the data, a sorption–desorption isotherm combination is generated by plotting the water uptake (% w/w) against %RH. A typical sorption–desorption isotherm is shown in Fig. 2. A sorption isotherm gives information about the water held in different forms at varying RHs. For example, water is held in the form of an adsorbed monolayer up to ~20 %RH, in the form of adsorbed multimolecular layers from ~20 to 65 %RH, and in the form of free water held in relatively large pores (capillary condensation) above 65 %RH. Water held by capillary condensation leads to a sharp increase in the swelling of the fiber. For most hydrophilic materials such as hair, water content as measured during desorption is higher than that during the sorption

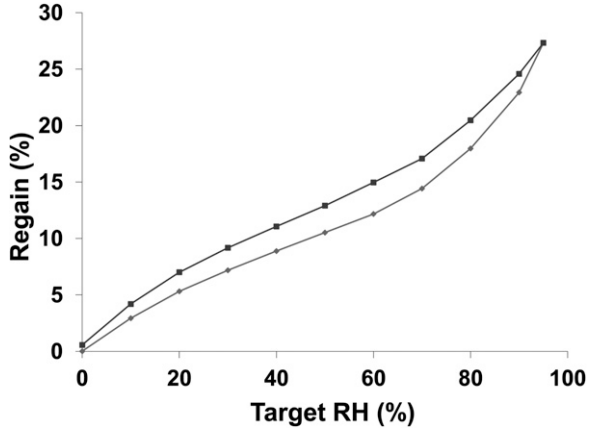

Figure 2. Sorption–desorption isotherm obtained using a dynamic vapor sorption analyzer (Surface Measurements Systems, Alperton, Middlesex, U.K.). Diamond symbols (bottom curve) corresponds to absorption and the square symbols (top curve) to desorption.

mode. This difference in the water uptake between desorption and sorption modes, known as sorption hysteresis, is characteristic of hydrophilic materials. The magnitude of this hysteresis depends on the detailed molecular structure and hydrophilicity.

Water uptake measurements provide information about the kinetics of water absorption, but not about distribution of water within the different morphological features of hair. This information can be derived from small-angle neutron scattering (SANS) obtained with water replaced by its equivalent deuterium oxide (D_2O) to achieve the scattering contrast. The scattered intensity at small scattering angles (2θ) contains information about large length-scale (10–100 nm, mesoscale) structures. Although structural information at these length scales can be obtained using X-rays (small-angle X-ray scattering, SAXS), neutrons provide unambiguous interpretation of the features that are accessible to water. This is because neutrons are scattered differently by hydrogen and deuterium. By replacing hydrogen with deuterium on polymer segments or host molecules, without altering the structure of the polymer or the interactions between the polymer and the host molecules, the distribution of these "colored" molecules can be imaged at large length scales (6). SANS measurements are mostly carried out with polymers that are specifically synthesized by replacing some of the hydrogen atoms with deuterium, a demanding task. However investigation of the diffusion of deuterated solvents into the polymer matrix is relatively simple. In this instance the contrast is generated by the distribution of the commercially available deuterated solvents, in our case deuterium oxide or heavy water, into the nondeuterated polymer. Note that with X-rays the scattering contrast is due to differences in electron density. Therefore, in a complex structure such as hair, changes in the scattering intensities in SAXS are due to both the electron density changes resulting from the presence of water and the changes in the structural features of the matrix itself. In SANS, it is possible to assign the features in the scattering pattern solely to structures associated with water (D_2O). Such work has been done on synthetic polyamides and starch (7,8). The data in Fig. 3, for instance, show the four broad diffraction spots generated by the presence of D_2O in the interlamellar spaces of a hydrated nylon fiber (9). A second feature in the SANS pattern, the diamond-shaped equatorial streak at the center of the pattern, is attributed to the water present in the longitudinal channels as well as from the surfaces of the fiber (10,11). We here carry out SANS

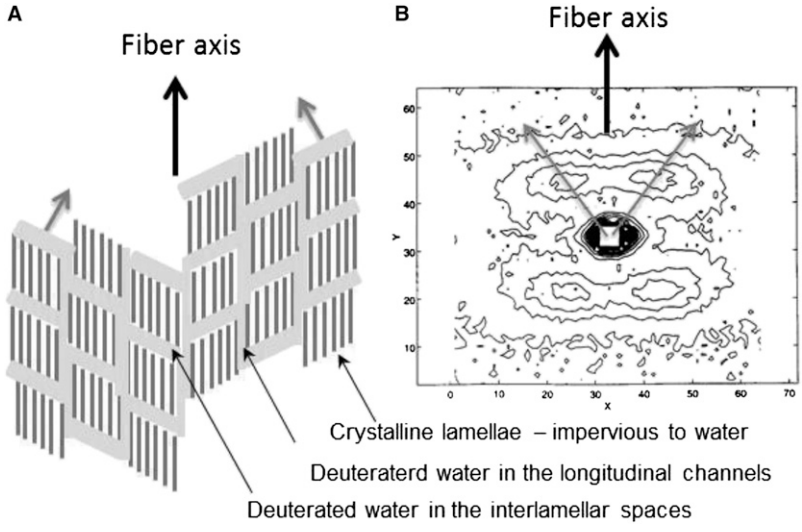

Figure 3. (A) Schematic illustration of the distribution of water in a fiber with crystalline and amorphous domains and (B) the resulting SANS pattern. Water in the interlamellar spaces gives rise to the meridional (fiber-axis) and off-meridional scattering. Water in the longitudinal channels contributes to the scattering along the equator (perpendicular to the fiber-axis).

measurements on several carefully prepared hair samples to see if similar distribution of water exists in hair. Infrared (IR) spectroscopy data are used to investigate the hydrogen–deuterium (H–D) exchange that occurs during saturation with D_2O.

EXPERIMENTAL

European dark brown hair (EDBH) obtained from International Hair Importers (Glendale, NY) was used in these experiments. Samples for SANS measurements were prepared by first removing the water in the hair by keeping them under vacuum for 24 h, and then equilibrating them for several days in D_2O atmosphere of desired humidity obtained using saturated salt solutions. A second set of samples were prepared by equilibrating them first with D_2O at the desired humidity for 24 h and then keeping the sample under vacuum at room temperature to remove free D_2O from the sample. For experiments designed to study the effect of oil, hair soaked with oil was prepared by treating the two tresses with oil (0.5 ml/g hair) followed by combing to spread the oil uniformly. One of the tresses was heat-treated for 90 s at 180°C. Both tresses were left overnight and then immersed in hexane for 30 s to remove surface oil. They were then equilibrated to the required humidity with solutions of salt and D_2O. Cuticle-free (CF) hair samples were also prepared using the CF hair supplied as special samples by International Hair Importers.

SANS data were collected on the CG-2 and CG-3 beam lines at the Oak Ridge National Laboratory (Oak Ridge, TN). The q-range was between 0.05 and 0.025 nm^{-1}. The data were normalized to tress thickness. Hair aligned in the form of a thin tress (~2–3 mm in thickness and ~15 mm in width) was mounted on U-frames made of aluminum plate using superglue. These plates were placed in airtight cells to maintain the samples at the required humidity. Different humidity levels were maintained using saturated solutions of appropriate salts in water and D_2O. In the case of D_2O the RH is expressed as %RHD.

Attenuated total reflectance (ATR) spectra were collected using Nicolet 6700 FTIR (Thermo Electron Corporation, Madison WI). The respective hair sample was placed on the ATR crystal. The spectral region from 900 to 4000 cm^{-1} was scanned. Spectra were analyzed using OMNIC software (Thermo Electron Corporation).

RESULTS AND DISCUSSION

INTERNAL STRUCTURE OF HAIR

An example of the two-dimensional (2D) SANS pattern is shown in Fig. 4A. There is a key difference between Fig. 4A and Fig. 2 that was used for illustrating SANS. The dominant feature in Fig. 2 is attributed to the water in the interlamellar spaces, and is therefore aligned close to the fiber-axis (off-meridional). In contrast, the dominant feature in Fig. 4A is attributed to the water in the channels along the fiber-axis, and therefore occurs along the equator. We attribute the equatorial peak to the water in the spaces between the IFs. Only half of the scattering pattern was obtained so as to record the second maximum. This second peak is significantly weaker than the first. A one-dimensional intensity scan (I vs. q) perpendicular to the fiber-axes obtained from this image is plotted in Fig. 4B. Here, q is the scattering vector defined as

$$q = 4\pi \sin\theta/\lambda \tag{1}$$

where λ is the wavelength of the neutrons (0.478 nm) and 2θ is the scattering angle. The spacing (d) between the scattering entities is calculated by Bragg's equation

$$d = 2\pi /q \tag{2}$$

The large scattering intensity, shown in dark (or red) color in Fig. 4A, arises from both the contrast due to D_2O and due to the H–D exchange in the amine and amide groups in the hair structure. As shown using the IR data in a later section, the water taken up initially is strongly adsorbed, or even exchanged between the amine and amide functionality of the protein.

The changes in the SANS intensity with the D_2O concentration in hair can be understood by considering the changes in the contrast in the dry and the D_2O-wet hair. Because hydrogen has negative scattering length, there is a small negative contrast in the dry samples. As shown later in the section on CF hair, this negative contrast gives rise to a SANS interference peak even in dry samples. With infusion of some D_2O, this contrast disappears at <6 %RHD, and the scattered intensity approaches zero. As the hair continues to absorb more D_2O, contrast reaches large positive values and the intensity increases considerably.

The interference peaks at q = 0.07 $Å^{-1}$, the dumbbell-like pattern, and a weaker peak at 0.13 $Å^{-1}$ are evidence of D_2O diffusing into the matrix between the IFs, as well as into the IFs. The d-spacing corresponding to the peak at q = 0.07 $Å^{-1}$ in Fig. 4B is 95 Å. This is consistent with 75 Å size of the IF (Fig. 1B). The second weak peak at q ~0.13 $Å^{-1}$ (d = 48 Å) has contributions from the internal structure and from the lipids in keratinous tissue (12,13). Although it was claimed that the presence of this ring could be used to diagnose breast cancer (14), this was later refuted (13). Consistent with these latter papers, our study data show that the 0.13 $Å^{-1}$ peak is a composite of the second order of reflection from IF assembly and from the lipids (to be published).

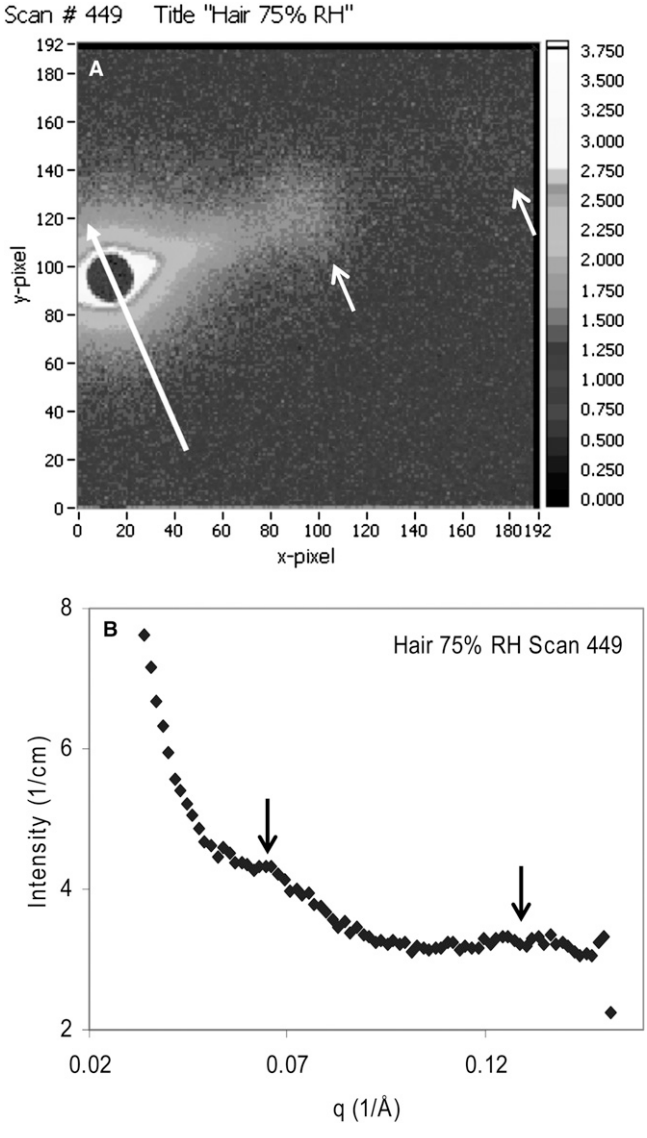

Figure 4. (A) A typical 2D small-angle neutron scattering from a hair sample. The dark spot is the shadow of beam stop that blocks the main beam. Side bar shows the intensity scale. The large arrow indicates the direction of alignment of hair fibers. The two small arrows indicate the two interference peaks. These data were obtained from a hair tress equilibrated at 75 %RHD; (B) one-dimensional (1D) intensity scan as a function of scattering vector obtained from the 2D image by summing the intensity along a slice perpendicular the fiber-axis.

Given that both the interference peaks (q ~0.07 and 0.13 $Å^{-1}$) arise from the organization of the intermediate and protofilaments, we would expect that as the hair takes up moisture and swells at the macroscopic level, there would be swelling of the structures at the level of IFs as well. This was indeed observed as the interference peaks ("dumbbells" spots in Fig. 4A) move inwards, corresponding to an increase in the d-spacing from 95 to 101 Å as the humidity is increased from 32 to 92 %RH.

One observation in this study is that the scattering intensity corresponding to q = 0.07 and 0.13 $Å^{-1}$ did not change significantly with the amount of water (D_2O) in the sample after the first hydration up to 50 %RH. This suggests that the fraction of water in the vicinity of the IFs in the cortical cells remains relatively constant over the 50–95% humidity range. This was also reflected in the increase in the *d*-spacings. The increase in the *d*-spacings corresponds to a swelling of ~13%. However, Fig. 3 shows that the amount of water absorbed reaches 12% at 50 %RH, and then accelerates to reach value of ~25% as the humidity is increased to 95%. As amount of absorbed water increases with humidity, it shows that the additional water is present in regions other than the IF assemblies. The amount of water in these regions is expected to be different from that bound to the amide groups in the protein matrix. These assertions are supported by depolarization thermal-current (DTC) study in which ice-like water was reported at 19% water content (15). This water does not have the rotational properties of free water but has the polarization properties of the water molecules in the liquid state. Note that the 19% water content at which this new water peak appears in the DTC study is about the same value at which the amount of water accelerates in sorption isotherm experiments (Fig. 2). The central diffuse scattering (CDS) observed near the beam stop suggests that water could be present in mesoporous (void structures between 100 and 1000 nm in size) regions in hair. Preliminary results in fact show a decrease in this intensity in hair exposed to D_2O, perhaps because of contrast matching. More than one structural feature contributes to the CDS (16). Important among these are the refraction from the macroscopic surfaces (hair) and microscopic surfaces (internal structure) (10), microvoids within the hair, and fibrils. Because the surface scattering and refraction from surfaces appear in the form of elongated streaks (10), absence of such elongated streaks along the equator allows us to attribute the CDS to internal structures and microvoids within hair.

Although water sorption data can be used to determine the pore volume distribution in hair, it will not be accurate, because water swells the hair as it is absorbed, thus continually changing the pore size. Mercury intrusion porosimetry is commonly used for porosity determination. In this method, mercury is forced into the void structure of the fiber substrate under very high pressures (17). This method is generally not used for organic fibers because high pressures used deform the pore structure in the fiber. The standard method for determining the pore size distribution in solid substrates such as fibers is nitrogen adsorption at low temperatures, using Kelvin equation to convert the sorption data into pore volume (18). Gas adsorption measurements indeed show that pores are present in hair, and their distribution changes during various hair treatments (19). The presence of pores is confirmed by recent detailed electron microscopy studies (20), atomic force microscopy studies (21), and optical measurements (22). Pores in the medullary features form a small fraction of the bulk of hair. Thus, water present in the keratinous structure gives rise to the interference peaks, and water present elsewhere, e.g., longitudinal pores, perhaps in the cortex and the cuticle, contributes to the CDS.

SANS OF CUTICLE-FREE HAIR

To determine if cuticular sheath is the locus of larger fraction of water in hair, we repeated the scattering experiments with CF hair. Samples of CF hair were prepared in the same way as regular hair as described earlier. Moisture-free samples of CF and regular EDBH were first prepared by keeping them under vacuum in the presence of phosphorous pentoxide. SANS patterns of the dry (no H_2O or D_2O) CF-free hair are shown in Fig. 5A.

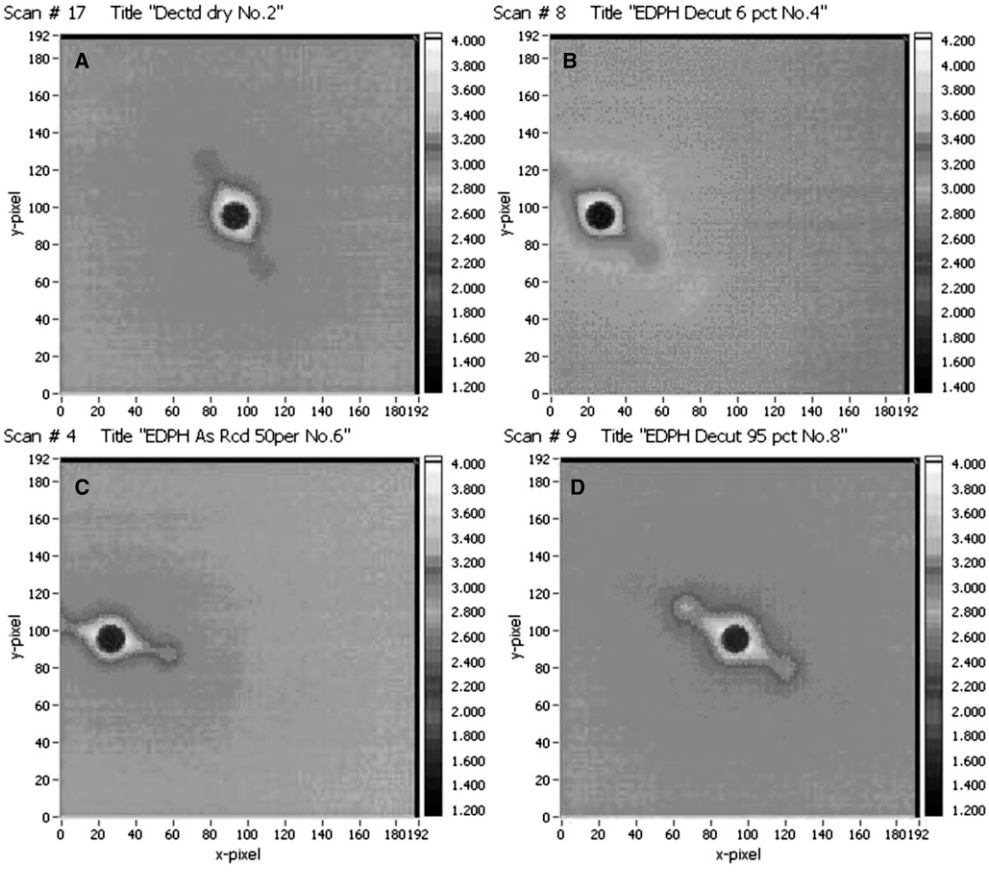

Figure 5. 2D SANS images of cuticle-free hair. The dark spot is the shadow of beam stop that blocks the main beam. Side bar shows the intensity scale. (A) Dry hair, (B) 6 %RHD, (C) 50 %RHD, and (D) 95 %RHD.

These patterns are similar to those of wet (D_2O) samples in Fig. 4 with a typical diamond-shaped halo around the beam stop and a faint dumbbell. The SANS images from these samples appear different because the data were collected under different instrument configurations. However, they provide the same information as the patterns in Fig. 4. SANS patterns from CF hair that were first placed in vacuum to remove water and then equilibrated with vapor of D_2O at 6, 50, and 95 %RHDs are shown in Figs. 5B–D. The intensity is enhanced at 50 and 95 %RHD because of the presence of D_2O, indicating significant amounts of water diffusing into the matrix. The scattered intensity in both the as-received and the CF hair are quite similar. This suggests that cuticle sheath does not hold any significant amount of water, and that most of the water is present in the medullary and the microfibril regions of the hair.

ABSORPTION OF OIL IN HAIR

Earlier studies have shown a greater permeation of saturated vegetable oils such as coconut oil into hair than the polyunsaturated oils such as soybean oil (23). Heat treatment

at high temperature often promotes the penetration of the oil deeper into the fiber. To understand the mechanism of oil diffusion into the hair's hierarchical structure, we prepared four tresses as mentioned in the experimental section. The SANS patterns of these tresses are shown in Fig. 6. The interference peaks are more intense in the heat-treated hair in both the coconut and the soybean oil-treated hairs, suggesting that more water present in the spaces between the IFs. This shows that heat treatment opens up additional pathways, perhaps through the formation of new pores, for water to diffuse into the cortical regions of the hair. Detailed analysis (to be published) also showed that the interference peaks, both in the sample kept at room temperature and in the heat-treated sample, were stronger in the soybean oil-saturated hair than in the coconut oil-treated hair under the same conditions. This suggests that this diffusion-blocking effect is weaker with soybean oil than with coconut oil. This could be because of smaller amount of soybean oil penetrates into the fiber and thus blocks fewer pathways for penetration of water than coconut oil (24). These results show that SANS is a useful technique for studying substrates that have been rendered hydrophobic by oil or other treatments, which block diffusion of water.

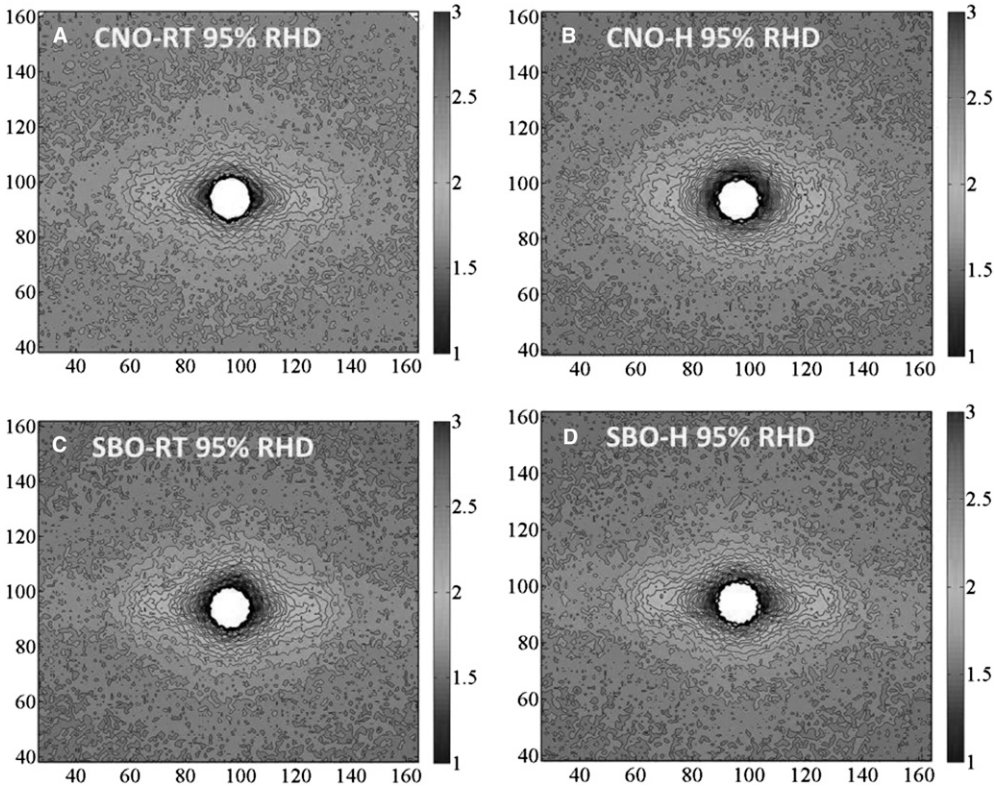

Figure 6. 2D SANS images of hair treated with oil. The dark spot is the shadow of beam stop that blocks the main beam. Side bar shows the intensity scale. (A) Coconut oil—before heat treatment, (B) coconut oil—after heat treatment, (C) soybean oil—before heat treatment, and (D) soybean oil—after heat treatment. All at 90 %RHD.

H⇔D EXCHANGE EFFECT OF D_2O DIFFUSION INTO HAIR

Polymeric substrates capable of hydrogen bonding with water when treated with D_2O undergo H⇔D exchange. Upon drying, this leaves some residual D in the sample. In hair, H⇔D exchange can occur at pendant $–NH_2$ (as in amino acid lysine as well as –CONH– functionalities), as shown by the following two schemes.

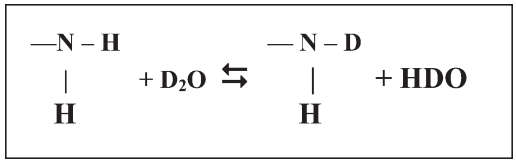

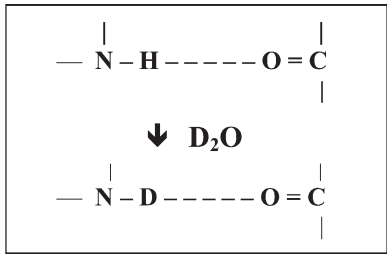

The possibility of such exchange can be studied by infrared spectroscopy [Fourier transform infrared spectroscopy (FTIR) mode]. As the reduced mass increases when H⇔D exchange occurs at N, both stretching and bending frequencies will be reduced significantly. For example, N–H frequency of the amine group (3219 cm^{-1}) will be reduced to 2420 cm^{-1}. But this frequency could not be followed in our experiments as it overlaps with that of CO_2, and thus can be observed only with an FTIR spectrometer that can be flushed with nitrogen. Instead, we followed the bending frequencies of the amide functionality (amides I and II) (1632 and 1516 cm^{-1}, respectively). FTIR spectra of H⇔D exchange in hair are shown in Fig. 7A. The figure shows that the amide II peak shifts down with the substitution of H with D as expected. Treating this sample with water at 55°C should reverse this shift; however, this was not observed although Murthy *et al*. (7) reported such a shift at this temperature following the deuterated amine end groups in nylon. In the present work, this reversal was observed only after treating the sample with boiling water (100°C). This can be seen in Fig. 7B that shows the upshift of the amide II peak following the substitution of D with H.

CONCLUSIONS

This preliminary SANS study of human hair has shown that water is present in essentially two forms: one that is adsorbed through hydrogen bonding and exchanged with amine and amide nitrogen in the spaces between the IFs and protofilaments, and the other in mesoporous regions as multimolecular layers and free D_2O. Analysis of the interference peak due to water in the filamentary regions gives the spacing between the IFs to be 95 Å. A weak second-order

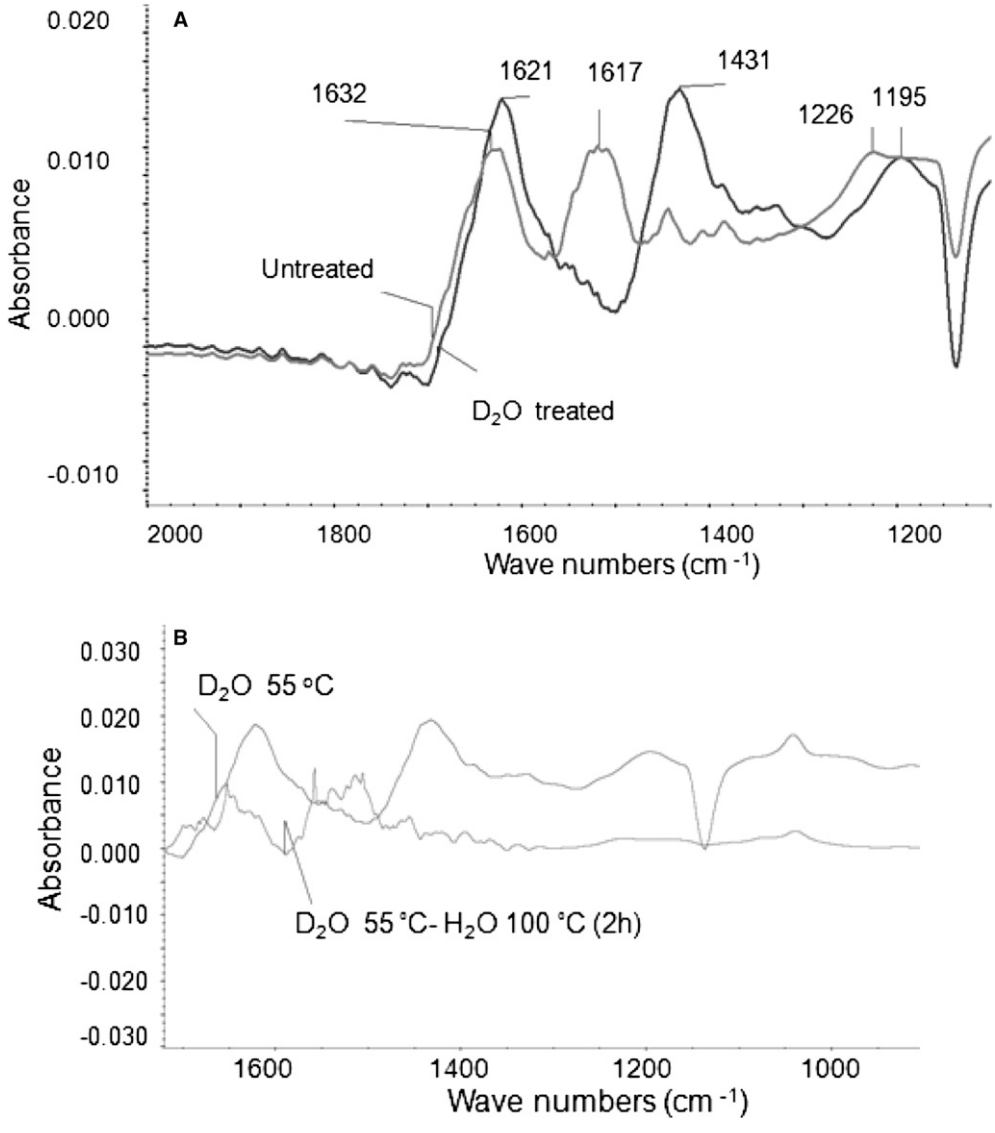

Figure 7. IR spectra of hair. (A) Exposed to D_2O, and then (B) immersed in boiling water.

reflection in the diffraction pattern is attributed to the organization of the protofilaments in the cortical cells of hair. Amount of water in these regions of IFs appears to be relatively small compared to the total amount. A larger fraction of water appears to be present in the mesoporous regions, as indicated by the high-intensity near-zero scattering angles. Obvious features that correspond to the mesoporous entities in hair can be associated with the medullary structures, which are likely to be more hydrophilic and thus interact positively with water. Other mesoporous entities are the cracks generated by fiber damage, both in the cortex and the endocuticle region of the cuticle cell. Further SANS experiments with carefully prepared and well-characterized hair samples and analysis of the data could provide a detailed distribution of water in regions other than the IFs.

ACKNOWLEDGMENTS

These data were collected at beam lines CG-2 and CG-3 at the High Flux Isotope Reactor (HFIR) at the Oak Ridge National Laboratory. We thank Dr William Heller at HFIR for enabling the collection of the neutron scattering data, and Dr Wenjie Wang for processing some of the 2D data used in the figures.

REFERENCES

(1) E. Fuchs and D.W. Cleveland, A structural scaffolding of intermediate filaments in health and disease, *Science*, **279**, 514–519 (1998).
(2) C.R. Robbins, *Chemical and Physical Behavior of Human Hair*. (Springer-Verlag, New York, 1994).
(3) P. Jolles and H. Zahn, *Hair: Biology and Structure*. Vol. 78. (Birkhäuser, Basel, 1996).
(4) M. Feughelman, A two-phase structure for keratin fibers, *Text. Res. J.*, **29**, 223–228 (1959).
(5) C. Keis, C.L. Huemmer, and Y.K. Kamath, Effect of oil films on moisture vapor absorption on human hair, *J. Cosmet. Sci.*, **58**, 135–146 (2007).
(6) G.D. Wignall, "Small-angle-neutron-scattering characterization of polymers," in *Physical Properties of Polymers*. (Cambridge University Press, Cambridge, U.K., 1993), pp. 424–511.
(7) N.S. Murthy, M. Stamm, J.P. Sibilia, and S. Krimm, Structural changes accompanying hydration in nylon 6, *Macromolecules*, **22**, 1261–1267 (1989).
(8) J. Blazek and E.P. Gilbert, Application of small-angle X-ray and neutron scattering techniques to the characterisation of starch structure: A review, *Carbohydr. Polym.*, **85**, 281–293 (2011).
(9) N.S. Murthy, Fibrillar structure and its relevance to diffusion, shrinkage, and relaxation processes in nylon fibers1, *Text. Res. J.*, **67**, 511–520 (1997).
(10) D.T. Grubb and N.S. Murthy, Real-time X-ray study of nylon-6 fibers during dehydration: Equatorial small-angle scattering is due to surface refraction, *Macromolecules*, **43**, 1016–1027 (2009).
(11) N.S. Murthy and W.J. Orts, Hydration in semicrystalline polymers: Small-angle neutron scattering studies of the effect of drawing in nylon-6 fibers, *J. Polym. Sci. Part B: Polym. Phys.*, **32**, 2695–2703 (1994).
(12) M.E. Rafik, F. Briki, M. Burghammer, and J. Doucet, In vivo formation steps of the hard α-keratin intermediate filament along a hair follicle: Evidence for structural polymorphism, *J. Struct. Biol.*, **154**, 79–88 (2006).
(13) F. Briki, B. Busson, B. Salicru, F. Estève, and J. Doucet, Breast-cancer diagnosis using hair, *Nature*, **400**, 226 (1999).
(14) V. James, J. Kearsley, T. Irving, Y. Amemiya, and D. Cookson, Using hair to screen for breast cancer, *Nature*, **398**, 33 (1999).
(15) J.L. Leveque, J.C. Garson, P. Pissis, and G. Boudouris, Free water in hair keratin? A depolarization thermal-current study, *Biopolymers*, **20**, 2649–2656 (1981).
(16) W. Wang, N.S. Murthy, and D.T. Grubb, Central small-angle diffuse scattering from fibers is made of two components, *J. Polym. Sci. Part B: Polym. Phys.*, **50**, 797–804 (2012).
(17) R.G. Quynn, Internal volume in fibers, *Text. Res. J.*, **33**, 21–34 (1963).
(18) P.H. Emmett, Adsorption and pore-size measurements on charcoals and whetlerites, *Chem. Rev.*, **43**, 69–148 (1948).
(19) Y.Z. Hessefort, B.T. Holland, and R.W. Cloud, True porosity measurement of hair: A new way to study hair damage mechanisms, *J. Cosmet. Sci.*, **59**, 303–315 (2008).
(20) R. De Cassia Comis Wagner, P.K. Kiyohara, M. Silveira, and I. Joekes, Electron microscopic observations of human hair medulla, *J. Microsc.*, **226**, 54–63 (2007).
(21) R.L. McMullen and S.P. Kelty, Investigation of human hair fibers using lateral force microscopy, *Scanning*, **23**, 337–345 (2001).
(22) S. Nagase, S. Shibuichi, E. Kariya, N. Satoh, and K. Ando, Influence of internal structures of hair fiber on hair appearance. I. Light scattering from the porous structure of the medulla of human hair, *J. Cosmet. Sci.*, **53**, 89–100 (2002).
(23) S.B. Ruetsch, Y.K. Kamath, A.S. Rele, and R.B. Mohile, Secondary ion mass spectrometric investigation of penetration of coconut and mineral oils into human hair fibers: Relevance to hair damage, *J. Cosmet. Sci.*, **52**, 169–184 (2001).
(24) S.B. Hornby, Y. Appa, S.Ruetsch, and Y. Kamath, Mapping penetration of cosmetic compounds into hair fibers using time of flight secondary ion mass spectroscopy (TOF–SIMS), *IFSCC Magazine*, **8**, 99–104 (2005).